Università di Pisa SSD: CHIM/02

School of Graduate Studies G. Galilei

PhD Thesis in Chemical Science

Study of organic molecules in their crystalline phases by Solid State NMR: dynamics and related aspects

Elisa Carignani

Supervisor

Dr. Marco Geppi

Advisors

Prof. Robin K. Harris Prof. Steven P. Brown

Pisa, January 2013

Introduction

The study of molecular dynamic properties has a fundamental interest from a physico-chemical point of view and can give crucial information about the molecular origin of several macroscopic properties. For instance, besides other aspects, solids and liquids differ by the degree of freedom of the molecules in the two physical states: in the liquid state the whole molecules undergo fast translational and rotational motions, which, on the contrary, are absent in the solid state. Actually, with the only exception of the so-called plastic crystals in which rotations of the whole molecules are present, in a crystalline phase the molecules have a fixed position and orientation. However, this does not imply the absence of dynamic processes in the solid state, where, as it is well known, internal molecular motions can occur, in addition to vibrations and librations that are always present.

In particular, the study of molecular motions of small organic molecules in the solid state has a considerable interest, not only for the intrinsic value of such a deep knowledge of a chemical system, but also because molecular motions can be intimately connected with physical properties, such as stability, intermolecular interactions and chemical reactivity [1]. Moreover solid-solid phase transitions are often triggered by the onset of an internal motion, and different polymorphs of the same compound are frequently characterized by a different dynamic behavior.

However, the identification and characterization of internal molecular motions is far from being trivial and only a few experimental techniques can give detailed and reliable dynamic information. Among them Solid State NMR (SSNMR) is the most versatile in terms of tools provided and it is the only one that allows

information to be obtained about the frequency, geometry and molecular fragments involved for each molecular motion [2, 3, 4, 5].

The power of SSNMR for the study of interconformational internal motions resides in the possibility of "observing" different nuclei and investigating several nuclear properties as well as in a number of external variables, such as temperature, Larmor frequency, and pulse amplitudes, which can be varied independently. These characteristics allow information to be obtained about motions with characteristic frequencies spanning over a wide range of (10^0−10^{11} Hz). In addition the possibility of studying different nuclei, and, thanks to high resolution techniques, different nuclear sites allows the localization of the motions over the molecular moieties. This is a very important feature that for instance distinguishes SSNMR techniques with respect to dielectric relaxation methods, the other important technique for dynamic studies.

Often the interpretation of SSNMR experimental data in terms of dynamic processes is not straightforward, but it requires the use of proper models in order to quantitatively analyze the effects of molecular motions on the NMR observables. Moreover, the combination of SSNMR and suitable computational methods is at present a very powerful approach for the characterization, not only of structural proprieties as proven by the development of "NMR crystallography" [6], but also for the study of molecular dynamics.

In this PhD thesis, the various tools offered by SSNMR have been intensively exploited in order to characterize in detail some peculiar aspects of the dynamic properties of small organic molecules in crystalline phases. The nuclei observed, ^{1}H and ^{13}C, present different characteristics of the two nuclear species often allowed complementary dynamic information to be obtained. A wide variety of nuclear observables has been investigated, ranging from isotropic and anisotropic chemical shifts, scalar and dipolar couplings, to different kinds of relaxation properties, by using many advanced SSNMR pulse sequences. The work is also characterized by the extension of the measurements over an unconventional range of temperatures, in particular some ^{13}C CP-MAS spectra have been acquired at temperatures down

to 20 K. Moreover the combination of measurements at different experimental frequencies was exploited in many cases. A last important feature of the thesis work is the use of many mathematical models for the data analysis. In particular the use of motional models for relaxation time analyses, like BBP and Cole-Cole models for spectral densities, the McConnell equations for modeling exchange motions, in some cases integrated with other models for the description of interference phenomena; finally the extension of a model firstly proposed by Wittebort et al. for the quantitative analysis of the effect of small-amplitude motions, such as vibrations and librations, on chemical shift tensors. In all the cases studied the aid of DFT calculations were shown to be very important and in some cases crucial.

The developed approaches were applied to four small organic molecules in crystalline phases, chosen for some similar chemical characteristics and for their pharmacological interest, since they are widely used non-steroidal anti-inflammatory drugs. The systems chosen are Ibuprofen, Sodium Ibuprofen, Naproxen and Sodium Naproxen, all of them in their stable crystalline phases.

In particular the thesis is organized into six chapters. In the first one the NMR framework is introduced, summarizing the theoretical background useful for the following discussion. In Chapter 2 the tools offered by SSNMR for the study of molecular motions are presented and those used in the thesis work are described, illustrating, together with the nuclear properties, the models necessary for the analysis.

All the experimental techniques used within the thesis work, are discussed in Chapter 3. In particular, the apparatuses used are described, with special attention to newly-developed equipments for low temperature measurements. Moreover, the pulse sequences applied for the measurements of all the nuclear properties of interest are schematically represented and briefly commented.

In Chapters 4-6, the application of the SSNMR experiments and theoretical models on four model systems aimed at characterizing and highlighting peculiar aspects of their dynamic behavior is described. Chapter 4 shows the detailed characterization of all the interconformational motions occurring in the di-hydrated

crystalline form of Sodium Ibuprofen over a range of temperature from 20 to 357 K. ^{13}C CP-MAS experiments, ^{13}C chemical shift tensors measurements, ^{1}H and ^{13}C T_1, and ^{1}H $T_{1\rho}$ measurements in the just mentioned temperature range have been performed. Through the combined analysis of all the data sets the interconformational motions have been individually and quantitatively characterized. In the last part of the chapter the behavior of the di-hydrated form is compared with that of the anhydrous form of Sodium Ibuprofen. In Chapter 5, the effects of small-amplitude vibrational motions on the ^{13}C chemical shift tensors of Ibuprofen are discussed. Following a preliminary study, first the interconformational motions were analyzed and in particular the π-flip of the aromatic ring was found to have a characteristic frequency lower than 100 Hz at room temperature. This allowed the sole effects of vibrations and librations of this molecular fragment to be investigated, through a new method based on the comparison between experimental and DFT calculated chemical shift tensors. In this chapter, the model developed and the results obtained are presented, and finally a validation of the method by low temperature measurements is shown. In the last chapter (Chapter 6) the study of Naproxen and Sodium Naproxen is presented. In this case the interconformational motions are limited to the sole methyl and methoxyl rotations, which were quantitatively characterized by relaxation time measurements. Finally, the combination of advanced SSNMR experiments and DFT calculations allowed the assignment of all the resonances of the two compounds to be carried out, and in particular uncommon ring current effects on ^{1}H isotropic chemical shifts, arising from intermolecular interactions, to be identified and quantified.

Acknowledgments

This thesis wouldn't have been possible without the contribution of many people to whom I want to address my most sincere thanks.

Firstly, I would like to thank my supervisor Marco Geppi for the constant support, guidance, and trust he always showed to me. In these three years, and before, he provided me precious teachings and he has been a continuous source of good ideas and encouraging advices, all this is topped with an incredible passion for the job! I am really grateful to Silvia Borsacchi, without whom this thesis would not have been the same, for her continuos and invaluable help, deep expertise and warm smile. I have had a great support from all the present and former members of Marco's group: special thanks to Francesca for her help and our useful discussions, and an affectionate thank to Uma, both of them have been really special companions with whom I shared this experience. I would like to thank Sara and Elisa for the very good time spent together. All the people in the group have always showed to be special friends, and made this period very enjoyable, as well as interesting and exciting. Thanks also to Giulia Mollica, a former member of the group who has been very important in the development of this research line, for all her work in this field.

Among the "NMR people" in Pisa, I would like to thank Lucia Calucci, for being always available for any help, Claudia Forte, for the interest showed for the work, and Donata Catalano, for having introduced me in the NMR world much before the beginning of this thesis. A special thought goes to Alberto who I miss a lot.

An important part of the thesis have been done in the laboratory of prof. Malcolm Levitt at the University of Southampton: I would like to thank him firstly for having given me the opportunity of working with the unique cryo-equipment (and cryo-staff) in Southampton, and also for having welcomed me in his group for six very enjoyable months. Among the cryo-staff, I am very grateful to Maria Concistrè for being a guide in this period, for all her teachings and the constant side-by-side work with me, in the daily and nightly running. I wish also to thank Ole Johannessen for his technical support during the experiments and for his tireless work in setting up the experimental equipment. Moreover, thanks to Salvatore Mamone and Giuseppe Pileio for their availability and help in many situations. Thanks to all the members of the group for the nice and friendly atmosphere. There is a small group of people who made this period a unique and surprising adventure, I want to address a special thank to Maria and Peppe, for their hospitality and the special friendship they showed from the first day, and I would like to thank Rosa and Gerardo for their cheerfulness and help in any moment... And thanks to you four for the great time spent together!

I am linked to England also for another part of the work, for this I would like to thank prof. Steven Brown who gave me the opportunity of spending three weeks in his lab at the University of Warwick and of learning new techniques. I would like to thank especially Jonathan Bradley, who taught me many things and helped me in all the work done in this period, and thanks to the whole big SSNMR group in Warwick. Beside the scientific point of you I would like to thank Jonathan again, Ruth and Catharine for their kindness and hospitality.

Moreover, I would like to thank prof. Robin Harris for having been a careful and punctual advisor.

For a strong collaboration in these three years, I would like to thank prof. Benedetta Mennucci (Università di Pisa) and Alberto Marini, who helped at the beginning of this collaboration.

I would also like to thank prof. Paola Paoli (Università di Firenze), Patrizia Rossi and Eleonora Macedi, of her group, for their availability and the considerable

work done within our collaboration.

Outside chemistry, I think of many friends that were close to me in these three years, I want to thank all of them and in particular Sara and Veronica.

I want to thank my big big family, they were always interested in my work and I felt their support in any moment, especially when I was abroad. Particular thanks to my Mum and Dad, always proud of my work: they accepted and supported my path in these three years, wherever it would have taken me. I could not have done all this work without the encouragement of my sister Giulia, and my brothers Michele and Uberto: they always understood and helped me to see everything in the right perspective.

Last but not least I wish to thank you, Stefano, for putting up with me, especially in the writing period, and always taking care of me.

Contents

Chapter 1

Basic Principles of Solid State NMR

Nuclear Magnetic Resonance (NMR) spectroscopy [7] exploits the magnetic and electric interactions occurring between nuclear spins and different electromagnetic fields, either artificially applied or caused by the surrounding nuclei and electrons. The NMR phenomenon can be described with different theoretical approaches: many of the principal aspects connected to the dynamics of non-interacting nuclear spins can be treated with the vectorial model, based on the concept of classical angular momentum, but when the interaction among the spins of the sample are taken into account, the Quantum Mechanical (QM) model is often required. In this chapter only some elements of the QM model, which are relevant to this work, will be defined and briefly discussed, referring to fundamental literature for a complete theoretical treatment.

Within the QM model, the Zeeman states are defined as eigenstates of the Hamiltonian that describes the interactions of the nuclear spins with the static external magnetic field, and the evolution of the superposition states is described by the time-dependent Schrödinger equation. The resolution of time-dependent Schrödinger equation is strongly dependent on the complexity of the spin systems and the nature of the Hamiltonian. In any case, first of all the wave function and

the Hamiltonian operator have to be defined and analytically expressed. In the next sections, these two issues will be considered.

1.1 The density operator

As far as the wave function is concerned, the treatment is simple when a single spin is taken into account. In this case, any superposition state of the nuclear spin can be expressed as a linear combination of the Zeeman eigenstates, with the form, for spin-$\frac{1}{2}$:

$$|\psi\rangle = C_\alpha|\alpha\rangle + C_\beta|\beta\rangle \tag{1.1}$$

On the contrary, when a macroscopic sample constituted by many spins is taken into account the treatment is more complex. The QM description of the spin ensemble in this case would require to consider each individual spin and add their contribution together. In order to avoid to refer to the states of the individual nuclear spins, the *density operator* formalism [8, 9, 10] has been developed. Following this approach, the real system is described as a statistical ensemble of non-interacting spin systems, each constituted by N interacting spins. The density operator for the ensemble has the form:

$$\hat{\rho}(t) = \overline{|\psi\rangle\langle\psi|} \tag{1.2}$$

where the overbar indicates the average over all members of the ensemble, and the dependence on the time is implicit in the ψ function. The density operator expressed in the Zeeman eigenbasis is given by the following:

$$\hat{\rho}(t) = \sum_{r,s} \rho_{rs}(t)|r\rangle\langle s| \tag{1.3}$$

where $|r\rangle$ and $|s\rangle$ are the Zeeman eigenstates and $\rho_{rs}(t)$ are the matrix elements of the density operator:

$$\rho_{rs}(t) = \langle r|\rho(t)|s\rangle \tag{1.4}$$

The diagonal elements ($r = s$) of the spin density matrix are called *populations* of the corresponding states $|r\rangle$. The off-diagonal elements ($r \neq s$) are called *coherences* between the states $|r\rangle$ and $|s\rangle$.

The operator $|r\rangle\langle s|$, associated to the coherence ρ_{rs}, and the spin operator $\hat{S}_z$ are related by the following equation:

$$[\hat{S}_z, |r\rangle\langle s|] = p_{rs}|r\rangle\langle s| \tag{1.5}$$

where

$$p_{rs} = m_r - m_s \tag{1.6}$$

is the *coherence order* and m_r is the eigenvalue of the operator $\hat{S}_z$ in the Zeeman eigenbasis. A zero-quantum (ZQ) coherence corresponds to a spin operator connecting two spin states $|r\rangle$ and $|s\rangle$ for which $p_{rs} = 0$, while single-quantum and double-quantum coherences correspond to $p_{rs} = 1$ and $p_{rs} = 2$ respectively.

The expectation value of an observable Q of the spin system can be calculated by the density operator as:

$$\langle Q\rangle = Tr\{\hat{\rho}(t)Q\} \tag{1.7}$$

When a perturbation is applied to the spin system, the perturbator generally being $\hat{\mathcal{H}}$, a time-dependent evolution of the density operator is produced and can be described by the Liouville-von Neuman equation [10]:

$$\frac{d}{dt}\hat{\rho}(t) = -i[\hat{\mathcal{H}}(t), \hat{\rho}(t)] \tag{1.8}$$

as the equation of motion where $\hat{\rho}(t)$ and $\hat{\mathcal{H}}(t)$ denote the density operator and the Hamiltonian, respectively, at time t.

NMR experiments can be described using the Liouville-von Neuman equation, but in general, when a time dependent operator acts on the spin system the equation cannot be solved analytically. In this case different approaches can be used

in order to find an approximated solution, the most used for analyzing Solid State NMR experiments being the *average Hamiltonian* [10] and *Floquet Theory* [11].

1.2 Nuclear spin Hamiltonian in the solid state

The total nuclear spin Hamiltonian can be at first divided into two main contributions:

$$\hat{\mathcal{H}}(t) = \hat{\mathcal{H}}_{ext}(t) + \hat{\mathcal{H}}_{int}(t) \tag{1.9}$$

where the first term ($\hat{\mathcal{H}}_{ext}$) represent external contributions from the interaction with the static magnetic field (Zeeman interaction) and with the radiofrequency (rf)) field. In the laboratory frame, $\hat{\mathcal{H}}_{ext}$ takes the form:

$$\hat{\mathcal{H}}_{ext}(t) = \hat{\mathcal{H}}_Z + \hat{\mathcal{H}}_{rf}(t) = \omega_0 \hat{I}_z + 2\omega_{rf} cos(\omega_c t + \phi)\hat{I}_x \tag{1.10}$$

where γ is the gyromagnetic ratio of the observed nucleus, B_{rf} is the magnetic field connected with the radiofrequency, $\omega_{rf} = -\gamma B_{rf}$, ω_c and ϕ denotes the amplitude (angular frequency), and the phase of the rf field, respectively.

$\hat{\mathcal{H}}_{int}$ contains parts of the nuclear spin Hamiltonian that described the so-called "Internal interactions" of the spin system, and can be divided into the contributions of several interactions. For a diamagnetic system the internal Hamiltonian essentially consists of:

$$\hat{\mathcal{H}}_{int}(t) = \hat{\mathcal{H}}_S(t) + \hat{\mathcal{H}}_D(t) + \hat{\mathcal{H}}_J(t) + \hat{\mathcal{H}}_Q(t) \tag{1.11}$$

where the different terms of the Hamiltonian refer to different interactions:

$\hat{\mathcal{H}}_{CS}$ Shielding interaction,

$\hat{\mathcal{H}}_D$ direct Dipole-Dipole coupling,

$\hat{\mathcal{H}}_J$ Scalar coupling (J-coupling),

$\hat{\mathcal{H}}_Q$ Quadrupolar coupling.

In the large majority of the cases the Zeeman interaction is much more intense than the internal interactions. When this condition is true, the perturbation theory can be applied, being the Zeeman Hamiltonian the zero non-perturbated term and all the other interactions can be treated as first order perturbative corrections. The first order corrections to the eigenvalues exclusively depend on the secular part of the interaction Hamiltonian, *i.e.* the part commuting with $\hat{\mathcal{H}}_Z$. For the purposes of the present thesis the secular approximation is always valid and the following treatment is limited to this approximation.

1.3 Axes frames and rotations

All the internal interaction Hamiltonians can be expressed in cartesian or spherical tensorial forms, and the different tensors can be conveniently described in different axes frames. In the following a small introduction to the different axes frames used in the thesis work and the rotations among them is presented (Figure 1.1).

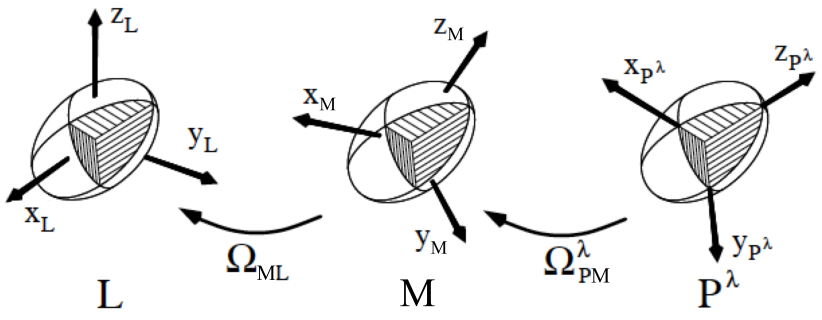

Figure 1.1: Representation of an interaction tensor λ in three different axes frames: the Principal axes frame (P), the molecular frame (M) and the laboratory frame (L). Ω_{IJ} indicates Euler angles describing the orientation between the system I and J.

- The *Laboratory Frame*, indicated with L, is a Cartesian frame in which the

$\vec{Z}_L$ axis lies along the static magnetic field $\vec{B}_0$.

- The *Molecular Frame*, indicated with M, is a Cartesian frame fixed on the molecule.
- The *Principal Axes Frame* of a particular interaction λ, indicated with P^λ, is a Cartesian frame, fixed on the molecular fragment, in which the tensor $\boldsymbol{\lambda}$ describing the interaction is diagonal.

A tensor can be rotated from one frame to another through an orthogonal transformation $R(\Omega_{IJ})$, Ω_{IJ} being the Euler angles specifying the orientation of the new reference frame (J) with respect to the initial reference frame (I). The tensor in the new frame can be expressed as

$$\boldsymbol{\lambda}_J = \mathbf{R}^{-1}(\Omega_{IJ})\ \boldsymbol{\lambda}_I\ \mathbf{R}(\Omega_{IJ}) \tag{1.12}$$

The convention adopted for Euler angles rotations is reported in appendix A.

1.4 Nuclear spin interactions

1.4.1 Shielding Interaction

The electrons in the molecules cause the local magnetic fields to vary on a *sub-molecular* distance scale. The effect that leads nuclei with different electronic environment to resonate at different frequency is called *shielding*.

The induced field, generated by molecular electrons, is, to a very good approximation, linearly dependent on the static external magnetic field ($\mathbf{B}_0$) and may be written as:

$$\mathbf{B}_j^{induced} = \boldsymbol{\sigma}_j \cdot \mathbf{B}_0 \tag{1.13}$$

where $\boldsymbol{\sigma}_j$ represents the *Shielding tensor* of the nuclear site j, which is a rank-2 cartesian tensor. The induced magnetic field usually is not in the same direction as $\mathbf{B}_0$, first because the induced field lines form closed loops and therefore they change orientation, and secondly because electrons circulate around axes defined by the peculiar three-dimensional shape of the molecules.

As for all the nuclear interactions, it is convenient to express the shielding tensor in its *Principal Axes Frame* (PAF) where the tensor is diagonal. In this thesis I will refer to the principal components of the absolute shielding tensor as σ_{11}, σ_{22} and σ_{33}, reported using the *standard notation*: $\sigma_{11} \leq \sigma_{22} \leq \sigma_{33}$ [12] (please note that the absolute shielding is referred to a nucleus in the vacuum without the presence of any electrons, see equation 1.18). The static lineshape due to the shielding interaction of a nucleus in a powder sample contains direct information on the principal components of the tensor $\boldsymbol{\sigma}$. The interesting frequencies are those in correspondence with the *shoulders* and the *divergence point*, represented in Figure 1.2, and are related with the principal components as follows:

$$\omega_{11} = \omega_0(1 - \sigma_{11}) \tag{1.14}$$

$$\omega_{22} = \omega_0(1 - \sigma_{22}) \tag{1.15}$$

$$\omega_{33} = \omega_0(1 - \sigma_{33}) \tag{1.16}$$

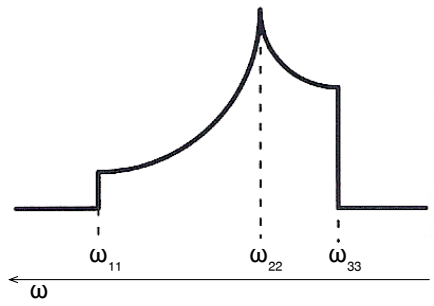

Figure 1.2: Lineshape due to the shielding interaction of a nucleus in a powder sample.

It is necessary to distinguish the shielding tensors, $\boldsymbol{\sigma}$, from the *Chemical Shift tensor*, $\boldsymbol{\delta}$; the latter also useful in many cases. The relationship between the principal components of the two tensors (δ_{ii} and σ_{ii}) is:

$$\delta_{ii} = \frac{\sigma_{ref} - \sigma_{ii}}{1 - \sigma_{ref}} \tag{1.17}$$

where σ_{ref} is the *absolute shielding* value of a reference compound, which is defined as:

$$\sigma_{ref}[\text{ppm}] = \frac{\nu_{nucl} - \nu}{\nu_{nucl}} 10^6 \tag{1.18}$$

being ν and ν_{nucl} the resonance frequency of the nucleus in the reference compound and in the vacuum without the presence of any electrons, respectively.

Usually $|\sigma_{ref}| \ll 1$, and equation 1.17 can be simplified in:

$$\delta_{ii} = \sigma_{ref} - \sigma_{ii} \tag{1.19}$$

From equation 1.19 is clear that within the standard notation the condition $\delta_{11} \geq \delta_{22} \geq \delta_{33}$ must be valid.

Shielding ($\boldsymbol{\sigma}$) and chemical shift ($\boldsymbol{\delta}$) tensors are expressed in the literature following different conventions, and sometimes the relationship between them is not clear. A rigorous description of the different conventions is present in Ref. [12].

1.4.2 Dipolar coupling

The *through-space* or *direct dipole-dipole* interaction corresponds to the classical coupling between magnetic dipoles. The direct dipolar coupling is mutual, and does not involve the electron clouds. Considering two nuclear spins (I and S), the Dipolar Hamiltonian is of the form:

$$\hat{\mathcal{H}}_D = -\left(\frac{\mu_0}{4\pi}\right)\gamma_I\gamma_S\hbar^2\left(\frac{\widehat{\boldsymbol{I}}\cdot\widehat{\boldsymbol{S}}}{r^3} - 3\frac{(\widehat{\boldsymbol{I}}\cdot\boldsymbol{r})(\widehat{\boldsymbol{S}}\cdot\boldsymbol{r})}{r^5}\right) \tag{1.20}$$

where $\hat{\boldsymbol{I}}$ and $\hat{\boldsymbol{S}}$ are the spin operators, and $\boldsymbol{r}$ is the internuclear vector.

In a cartesian tensorial form, analogue to the one used for the chemical shift, the dipolar interaction can be expressed as follows:

$$\hat{\mathcal{H}}_D = -2\hbar\ \hat{\boldsymbol{I}} \cdot \boldsymbol{D} \cdot \hat{\boldsymbol{S}} \tag{1.21}$$

where $\boldsymbol{D}$ is a rank-2 cartesian tensor, whose trace is always null and therefore its isotropic contribution, equal to $\frac{1}{3}Tr\boldsymbol{D}$, is null as well.

By expanding equation 1.20 and changing from cartesian to spherical coordinates, the dipolar Hamiltonian results:

$$\hat{\mathcal{H}}_D = -\left(\frac{\mu_0}{4\pi}\right)\frac{\gamma_I\gamma_S\hbar^2}{r^3}\left[\hat{A}+\hat{B}+\hat{C}+\hat{D}+\hat{E}+\hat{F}\right] \tag{1.22}$$

The terms $\hat{A}-\hat{F}$ (*dipolar alphabet*) are defined as:

$$\begin{aligned}
\hat{A} &= \hat{I}_z\hat{S}_z(3cos^2\theta-1)\\
\hat{B} &= -\frac{1}{4}[\hat{I}_+\hat{S}_- + \hat{I}_-\hat{S}_+](3cos^2\theta-1)\\
\hat{C} &= \frac{3}{2}[\hat{I}_z\hat{S}_+ + \hat{I}_+\hat{S}_z]sin\theta\ cos\theta\ e^{-i\phi}\\
\hat{D} &= \frac{3}{2}[\hat{I}_z\hat{S}_- + \hat{I}_-\hat{S}_z]sin\theta\ cos\theta\ e^{-i\phi}\\
\hat{E} &= \frac{3}{4}[\hat{I}_+\hat{S}_+]sin^2\theta\ e^{-2i\phi}\\
\hat{F} &= \frac{3}{4}[\hat{I}_-\hat{S}_-]sin^2\theta\ e^{-2i\phi}
\end{aligned} \tag{1.23}$$

where θ and ϕ are the polar coordinates describing the orientation of the vector $\boldsymbol{r}$ in the laboratory frame, and $\hat{I}_+,\ \hat{S}_+$ and $\hat{I}_-,\ \hat{S}_-$ are the *ladders operators*.

Following the perturbation theory, only the terms which commute with the Zeeman Hamiltonian contribute to the first order corrections. In the case of coupling between unlike spins (*heteronuclear coupling*, I $\neq$ S), the secular part is

represented by the A term only. This term solely involves the components of the magnetic moments along $\mathbf{B}_0$ and hence is responsible for the perturbation of the global energy of the spin system. Differently from the previous case, the secular part of the hamiltonian describing dipolar coupling between like spins (*homonuclear coupling*, I = S) contains the A and B terms. Contrary to A, the B term contains only the ladders operators, and therefore gives rise to energy-conserving flip-flop transitions.

1.4.3 Scalar coupling

The *scalar* or *J coupling* represents the magnetic interaction of nuclear spins with each other, through the involvement of bonding electrons, and hence, differently from the direct dipolar coupling, it is established only among chemically bonded nuclei. The corresponding Hamiltonian can be written as:

$$\mathcal{H}_J = \hbar\, \widehat{\boldsymbol{I}} \cdot \boldsymbol{J} \cdot \widehat{\boldsymbol{S}} \tag{1.24}$$

where the rank-2 tensor $\boldsymbol{J}$ has a non-null trace. For this reason the scalar coupling, as the chemical shift interaction, has an isotropic contribution. Since this term has usually a much smaller magnitude than the others, its effects are usually hidden by the larger linewidth produced by the anisotropic components of the other interactions present.

1.4.4 Quadrupolar interaction

Nuclei with spin $I > \frac{1}{2}$ have a non-spherical distribution of the charge producing an electric quadrupole moment that interacts with the electric field gradients originated by the nuclear and electronic charge distributions in their environment. This interaction is called *quadrupolar interaction* and, contrary to the interactions mentioned so far, possesses an electric nature. The quadrupolar Hamiltonian can be written in the form:

$$\hat{\mathcal{H}}_Q = \frac{eQ}{6I\,(2I-1)}\widehat{\boldsymbol{I}} \cdot \boldsymbol{V} \cdot \widehat{\boldsymbol{I}} \tag{1.25}$$

where Q is the nuclear quadrupolar moment and $\boldsymbol{V}$ is a rank-2 cartesian tensor that describes the electric field gradient acting on the nucleus. The elements of $\boldsymbol{V}$ have the following form:

$$V_{\alpha\beta} = \frac{\partial E_\alpha}{\partial r_\beta} \tag{1.26}$$

where $\alpha = x, y, z$ and $\beta = x, y, z$ are the spatial coordinates.

The tensor $\boldsymbol{V}$ is diagonal in its Principal Axes Frame (PAF). Using the principal components of the tensor, we can define two useful parameters:

$$\begin{aligned} eq &= V_{zz}^{PAF} \\ \eta_Q &= \frac{V_{xx}^{PAF} - V_{yy}^{PAF}}{V_{zz}^{PAF}} \end{aligned} \tag{1.27}$$

where e indicates the electric charge, eq is the *anisotropy* parameter of $\boldsymbol{V}$ and η_Q is the *asymmetry* parameter. Since the tensor $\boldsymbol{V}$ has a null trace, also the quadrupolar interaction, such as the dipolar one, does not have an isotropic contribution.

The quadrupolar interaction is the most intense of the spin interactions discussed so far: when its magnitude is not greater than $\sim \frac{1}{10}$ of the Zeeman term, a first order treatment is sufficient to describe the energy corrections, but when the entity of the interaction is larger, a second order correction to both the energy and eigenstates is needed [13].

The powder patterns calculated, with a first order treatment, for two cases ($I = 1$ and $I = \frac{3}{2}$), both with $\eta_Q = 0$, are shown in Figure 1.3.

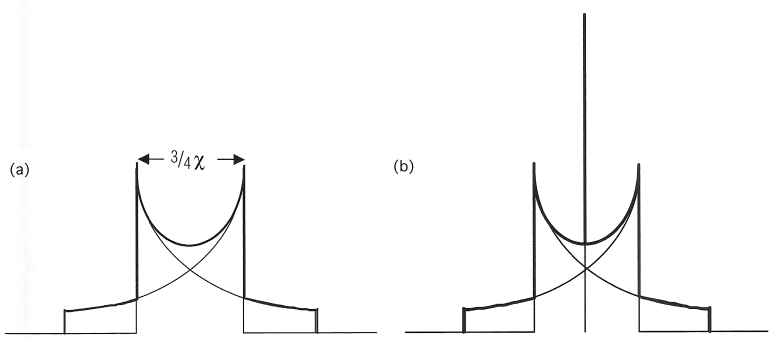

Figure 1.3: First order calculation of quadrupolar powder pattern for a nucleus with spin $I = 1$ (a) and $I = \frac{3}{2}(b)$. $\eta_Q = 0$ in both the cases, and χ is the quadrupolar constant (equal to $e^2qQ/\hbar$).

1.5 Nuclear spin relaxation

A spin system in a magnetic field reaches a state of thermal equilibrium when the populations of the spin levels obey the Boltzmann distribution and all the coherences are absent. After a perturbation, typically operated by radio frequency pulses, the system tends to regain the equilibrium state by means of *relaxation processes*. Two different kinds of relaxation are related to the movement of spin population back to their Boltzmann distribution and the decay of coherences: *spin-lattice relaxation* and *spin-spin relaxation*, respectively. Following the Bloch theory [7] the two types of relaxation can be treated independently.

Spin-lattice relaxation

The return of the populations to their equilibrium values is regulated by the spin-lattice relaxation process, which involves an exchange of energy between the system and the environment. Since this relaxation provides the longitudinal magnetization (that is along the z direction) to be recovered, it is also indicated as *longitudinal relaxation*. The time evolution of the longitudinal magnetization is usually regulated by an exponential law, whose time constant is T_1, called the *longitudinal* or *spin-lattice relaxation time*. A different spin-lattice relaxation can occur in solid

samples when the transverse magnetization is locked along the direction of the *rf* field in the rotating frame. In this case the transverse magnetization relaxes to zero with a mechanism called *spin-lattice relaxation in the rotating frame*, whose time constant is $T_{1\rho}$. Even if this kind of relaxation concerns the decay of transverse magnetization, it is classified in the spin-lattice relaxation mechanisms because it involves energy exchange with the lattice.

Spin-spin relaxation

The spin-spin relaxation concerns the decay of the coherences created by the *rf* field. This process involves an energy exchange among coupled spins and hence the total energy of the spin system does not vary but it is redistributed in the sample. Since this relaxation regulates the decay of the transverse magnetization it is also called *transverse relaxation*. The time constant is indicated as T_2, and it is called *spin-spin* or *transverse relaxation time*.

T_1, $T_{1\rho}$ and T_2 values contain important dynamic information and the analysis of their trend with temperature allows very detailed and often quantitative characterization of molecular motions to be obtained.

1.6 Spin diffusion

In solid samples the dipolar interaction plays a prevalent role in terms of magnitude with respect to the other interactions (except the quadrupolar one when present). A direct effect of the strong homonuclear dipolar coupling between abundant nuclei (typically ^{1}H, and ^{19}F in perfluorinated systems) is the *spin diffusion*, a phenomenon that consists in a spatial transfer of longitudinal magnetization between different sample areas. The $\hat{B}$ term of the homonuclear dipolar Hamiltonian $(I_+S_- + I_-S_+)$ is responsible for this phenomenon because it allows the so called *flip-flop* mechanism, *i.e.* an energy exchange between two nuclei keeping constant their total energy. For a pair of $I = \frac{1}{2}$ spins the flip-flop mechanism can be visu-

alized as a simultaneous inversion of the orientation of the two coupled magnetic moments with opposite spin orientation. Normally in a sample some protons have a stronger coupling with the lattice than others, and therefore have shorter T_1. In this way a magnetization gradient is generated between faster and slower relaxing areas. The longitudinal magnetization diffuse by means of the flip-flop mechanism from areas where the recovery is faster, called *relaxation sink*, towards those having a slower relaxation: resulting in a magnetization flux within the sample (Figure 1.4).

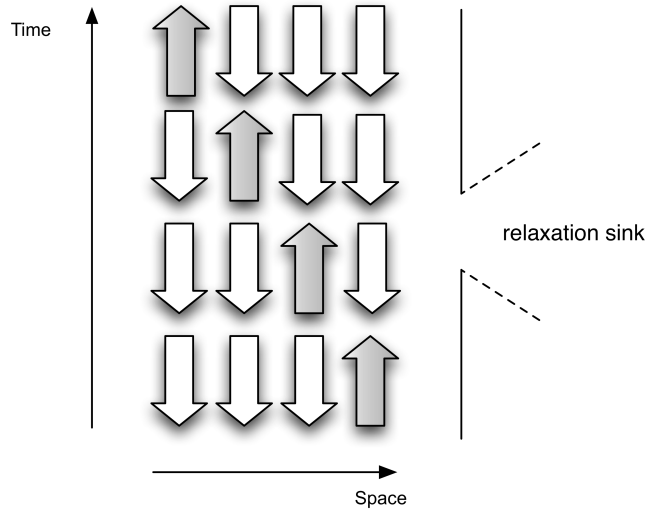

Figure 1.4: Representation of *spin diffusion* phenomenon. Through subsequent flip-flop transitions, the longitudinal magnetization diffuses from fast relaxing sample's zones to slower relaxing ones.

The spin diffusion occurs in the interval of time when longitudinal magnetization gradients are present in the sample, either naturally or after the application of suitable pulse sequences. As in the case of diffusion of matter, the time dependence of spin diffusion is governed by the Fick law:

$$\frac{\partial M(\boldsymbol{r},t)}{\partial t} = D(\boldsymbol{r})\nabla^2 M(\boldsymbol{r},t) \tag{1.28}$$

where M is the magnetization value in the position indicated by the vector $\boldsymbol{r}$,

and D is the diffusional coefficient. The equation 1.28 is valid when the local magnetization gradients are present, and the system evolves until, at a time τ, the gradients become zero. After the time τ, spin diffusion does not have further effects.

Spin diffusion affects T_1 and $T_{1\rho}$ values: every group of equivalent nuclei has intrinsic T_1 and $T_{1\rho}$ values in principle different from those of other groups of equivalent nuclei (non equivalent with those of the first group): spin diffusion tends to average the different intrinsic spin-lattice relaxation times to a single value. The average process can be complete, so a single value will be measured, or giving rise to observable partially averaged components. The effectiveness of the average depends on how long is the interval of time in which spin diffusion can operate. For example, for multi-phase materials a single value is obtained if the different phase domains do not have dimensions larger than $10 - 20$ Å and $100 - 200$ Å for $T_{1\rho}$ and T_1, respectively. This property makes this kind of study very useful for multi-component materials.

In all the cases, even when the average is not complete, spin diffusion effects prevent abundant nuclei spin-lattice relaxation times to be interpreted in terms of site-specific dynamical properties (which can be instead obtained from diluted spins relaxation times measurements), but they can still give precious information about the global dynamics of the sample.

Chapter 2

Effects of Molecular Dynamics on SSNMR Observables

Solid state NMR is a very powerful technique for the study of molecular dynamic properties: indeed, it can provide local and detailed information about molecular motions occurring in a very wide range of characteristic times (from 10^{-12} to 100 s). This ability arises from the possibility of exploiting all the nuclear spin interactions, which are anisotropic and therefore sensitive to the changes of orientation with time operated by molecular motions.

Moreover, the observation of different kinds of nuclei allows information on the different molecular fragments to be obtained. In particular, the observation of rare nuclei leads to site specific information relative to the molecular moiety which they belong to, while abundant nuclei generally give collective information about the whole molecule. The study of different nuclei, subjected to different interactions, gives complementary results from the spatial and temporal point of view.

Molecular motions are non-coherent processes, which can be described by *autocorrelation functions* $G(\tau)$:

$$G(\tau) = \overline{f(t)f(t+\tau)} \tag{2.1}$$

where $f(t)$ describes the time dependence of the molecular position or orientation with respect to the external magnetic field, and the overbar indicates the average over all the molecules in the sample.

The autocorrelation function value is a statistic measure of how much two orientations of a molecule (at time $t = 0$ and $t = \tau$) are correlated: if the motions are fast with respect to τ, a molecule statistically undergoes a significant orientation change in this interval of time, losing trace of the initial position: in this case the average of contributions with opposite sites gives a small value of $G(\tau)$. On the contrary, if the motions are slow, during τ the two orientations of the molecule will not change much, keeping trace of the initial position, and the contributions sum up positively giving a large value of $G(\tau)$ [9].

For stationary systems the autocorrelation function $G(\tau)$ depends only on τ, and in particular the function decreases as τ increase. Often the decay is assumed to be exponential:

$$G(\tau) = exp\left(-\frac{|\tau|}{\tau_c}\right) \tag{2.2}$$

where τ_c is the *correlation time* of the motion, a characteristic time that can coincide, for example, with a rotation period or the average time between two conformational jumps, depending on the geometry of the motion. A small value of τ_c corresponds to a fast motion and *viceversa*. Passing from the time to the frequency domain through the Fourier transform operation, the quantity $J(\omega)$, called *spectral density*, is obtained:

$$J(\omega) = \int G(\tau)\ e^{-i\omega\tau}\ d\tau \tag{2.3}$$

The spectral density functions are very useful quantities in the interpretation of NMR parameters in terms of dynamic processes.

The wide range of characteristic motional times accessible by SSNMR can be divided into three regimes:

Slow motional regime, $\tau_c > 10^{-3}$ s. The motions in this dynamic regime can

be studied by the *exchange experiments* in one or two dimensions.

Intermediate motional regime, $10^{-3} < \tau_c < 10^{-6}$ s. Motions with characteristic frequencies of the order of kHz can be investigated by means of *lineshape analysis* of the anisotropic patterns. The dynamic range to which the lineshape is sensitive depends on the kind of interaction under study. In particular each interaction is sensitive to motions with τ_c^{-1} of the order of the width of the static lineshape expressed in Hz. Information about motions in this regime can be obtained also from *transverse relaxation time* (T_2) measurements. Finally the motions with characteristic time in the intermediate regime can be studied by exploiting *spin-lattice relaxation times in the rotating frame*. $T_{1\rho}$ values are sensitive to motions with characteristic frequencies of the order of the *spin-lock* frequency, which is usually in the range 1-100 kHz.

Fast motional regime, $10^{-7} < \tau_c < 10^{-11}$ s. *Spin-lattice relaxation times in the laboratory frame* are a powerful tool for the characterization of motions in this regime. Indeed, T_1 values are determined by the fluctuations of nuclear spin interactions caused by molecular motions with frequencies of the order of the Larmor frequency.

Quadrupolar nuclei are rarely employed in dynamic studies, mostly because, as discussed in section 1.3, signal of nuclei with spin $> 1/2$ have a static linewidth, in the powder spectra, often of the order of MHz. This linewidth makes the observation of the signal difficult, thus preventing its use in dynamic studies. Deuterium represents a noticeable exception: ^{2}H nucleus has a spin number $I = 1$ and a quadrupolar moment relatively small, which gives rise to a quadrupolar coupling constant of the order of 140-220 kHz. This value makes it easily observable with respect to other quadrupolar nuclei [14]. In addition to lineshape analysis, deuterium has been exploited for relaxation time measurements and exchange experiments [13].

In the following sections, only the nuclear parameters used in the thesis work

will be described, together with their dependence on molecular dynamics and the methods used to extract information about molecular motions.

2.1 Effects of molecular motions on solid state NMR spectra

NMR experiments dedicated to dynamic studies are very powerful tools and allow detailed information about motional parameters to be obtained, but before discussing them it is really useful to consider how molecular motions can directly affect NMR spectra. Generally this could happen through exchange phenomena that affect the isotropic chemical shifts, and interference phenomena acting on the linewidth [15].

Average of anisotropic interactions

Very fast dynamic processes, *i.e.* with characteristic frequencies much larger than the linewidth of the interactions investigated, operate an average of the anisotropic components of those nuclear interactions. Such interactions are scaled by a factor that depends on the geometry of the motional process. For example, the molecule of adamatane in its crystalline solid form undergoes a fast reorientational motion, which have a strong effect in averaging the chemical shift anisotropy and the intramolecular dipolar couplings. However, the lack of translational freedom implies a scarce reduction of the intermolecular dipolar couplings. In SSNMR experiments adamantane behaves like a normal crystalline solid, but the proton dipolar coupling is reduced by a factor $\frac{1}{3}$. As a consequence NMR signals of adamantane are intrinsically narrower.

Chemical exchange effects on isotropic chemical shift

Molecular motions involving the exchange between two or more non equivalent nuclear sites affect the number, position and linewidth of the relative signals. In the case of two exchanging sites, the two signals are separated, each resonance frequency being the intrinsic one, when the characteristic frequency of the motion is lower than the difference of the two resonance frequencies expressed in Hz. On the contrary, if the characteristic frequency is much higher than the difference of the resonance frequencies, a single signal is present, centered at a frequency which is the average of the two intrinsic ones. Between these two situations, the coalescence occurs when the frequency of the motion is of the order of the difference of the two resonance frequencies.

In all the three situations, the shape of the spectrum can be simulated by using the solutions of the Mc Connell equations system [16]. In particular the observed spectrum corresponds to the sum of the imaginary parts of the solutions for the transverse magnetization of the two exchanging nuclei, M_A and M_B. The Mc Connell equations system shows the following form:

$$\begin{cases} iK - i(\omega - \omega_A)M_A - \frac{M_A}{T_2} + \frac{1}{\tau_c}(M_B - M_A) = 0 \\ \\ iK - i(\omega - \omega_B)M_B - \frac{M_B}{T_2} + \frac{1}{\tau_c}(M_A - M_B) = 0 \end{cases} \tag{2.4}$$

where K is a numeric constant, ω_A and ω_B are the intrinsic frequencies of the exchanging nuclei, τ_C is the correlation time of the motion and T_2 is the transverse relaxation time, assumed to be equal for the two sites.

The simulation of a series of spectra of two exchanging sites for different motional frequencies is shown in Figure 2.1.

A typical example of exchange motion is represented by the π flip of 1,4 disubstituted aromatic rings [17]. In this case the motion involves the exchange of two pairs of protonated carbons, and therefore in the spectra four distinct signals are present when the motion is slow, while only two signals are observed when the

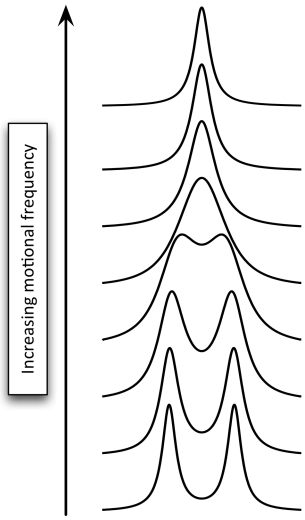

Figure 2.1: Effect of an exchange motion on the signals of two exchanging nuclei as a function of the motional frequency.

motion is fast.

Interference phenomena

Each molecular motion causes a modulation of the spin interactions according to its own frequency. Moreover, for the registration of high resolution spectra, external modulations are introduced too, associated for example with the MAS frequency or with external fluctuating magnetic fields, such as the spin lock or decoupling field.

The modulation due to a molecular motion can interfere with one of the instrumental frequencies, typically resulting in a linebroadening of the relevant signals, which depends on the value of the spectral density (Eq. 2.3) of the motion at the frequency of the external modulation.

Interferences with the MAS frequency can be observed when the dynamic processes have a characteristic frequency of the same order of magnitude (typically

1-50 kHz), that is when $J(\omega_{MAS})$ has a non-negligible value. In absence of motions, the evolution of the magnetization under the effect of anisotropic interactions and MAS rotation, gives rise to *spinning sidebands*, which are *rotor echoes* in the time domain. If the tensor of the interaction changes its orientation during a rotor period, because of molecular motions, the signal cannot focalize in the spinning sidebands. As a consequence, the FID decays much more rapidly and the signals experience a noticeable broadening.

The spectra of rare nuclei in the solid state are acquired under a strong decoupling field, preventing the broadening due to the heteronuclear dipolar coupling with abundant nuclei (generally protons). This is a further source of possible interference with molecular motions. Also in this case, when the frequencies of the motions are of the order of the decoupling frequency (typically 40-100 kHz), a linebroadening effect is observed.

The interference phenomena can be used for the characterization of molecular motions: for example, the frequency of the motion can be identified by varying the MAS or decoupling frequency at a fixed temperature, or, alternatively, with variable temperature experiments [18]. Indeed, the intrinsic linewidth of the signals is inversely proportional to the T_2 value. When the interference phenomenon occurs an additional contribution to T_2 (T_2^{int}) is created. And the total T_2^* can be calculated from the equation:

$$\frac{1}{T_2^*} = \frac{1}{T_2} + \frac{1}{T_2^{int}} \tag{2.5}$$

The dependence of T_2^{int} on the correlation time of the motion and on the interference frequency is expressed as follows [19]:

$$LW \propto \frac{1}{T_2^{int}} \propto \frac{2\tau}{1 + \omega_{int}^2 \tau_c^2} \tag{2.6}$$

The maximum linewidth is achieved when the following condition is verified:

$$\tau_c = \frac{1}{\omega_{int}} \tag{2.7}$$

where ω_{int} is the angular frequency of the external source of modulation, which interferes with molecular motions.

2.2 Lineshape analyses

The anisotropy of nuclear spin interactions produces, in powder samples, broad lines with a defined and characteristic profile for each chemically inequivalent site of the sample. For those interactions that give rise to a dishomogenous broadening, a pattern is ideally constituted by an infinite number of sharp lines, each one in correspondence of the frequency of a nucleus in a particular orientation with respect to the external magnetic field. A dynamic process that changes the molecule (or molecular fragment) orientation, causes an exchange between the lines corresponding to the different orientations, and therefore it results in a modification of the powder pattern.

If the characteristic frequency of the motion ($\nu_c = \tau_c^{-1}$) is of the same order of magnitude of the breadth of the static powder pattern, a *coalescence* occurs between the exchanging lines and the lineshape is distorted. Since the distortions depend on the geometry and frequency of the motion, they are a probe for the study of the dynamic process. Lineshapes can be simulated with appropriate theoretical models and by the comparison between experimental and simulated patterns the parameters of the motion can be determined [13].

2.2.1 Static lineshape simulation

When motions are absent, the time evolution of the net transverse magnetization (M^+) is governed by the equation:

$$\frac{dM^+(\theta,\phi;t)}{dt} = M^+(\theta,\phi)\,(i\omega(\theta,\phi) + T_2) \tag{2.8}$$

whose solution is the function:

$$M^+(\theta,\phi;t) = M_0^+(\theta,\phi)e^{(i\omega(\theta,\phi)t+T_2)} \tag{2.9}$$

where θ and ϕ describe the orientation of the external magnetic field $\boldsymbol{B_0}$ in a molecular axes frame. T_2 is the transverse relaxation time, $\omega(\theta,\phi)$ is the resonance frequency of a single orientation, and $M_0^+(\theta,\phi)$ is the intensity of the magnetization at $t = 0$ in the orientation described by θ and ϕ.

For a powder sample the total transverse magnetization can be obtained by an integration over all the possible orientations.

$$\begin{aligned} M^+(t) &= \frac{1}{8\pi^2}\int_0^{2\pi}\int_0^{\pi} M^+(\theta,\phi;t)\ sin\theta\ d\theta\ d\phi \\ &= \frac{1}{8\pi^2}\int_0^{2\pi}\int_0^{\pi} M_0^+(\theta,\phi)e^{(i\omega(\theta,\phi)t+T_2)}\ sin\theta\ d\theta\ d\phi \end{aligned} \tag{2.10}$$

In order to describe the effect of molecular motions on the time evolution of the transverse magnetization a model is needed. The most used for its simplicity and large applicability is the Markov model, which treats molecular motions as interconformational jumps between N discrete sites. An assumption of the model is that the time of the jumps is negligible with respect to the residence time in each site.

According to this model, equation 2.8 is modified as follows, in order to take into account the effect of the motion.

$$\frac{d\boldsymbol{M}^+(\theta,\phi;t)}{dt} = \boldsymbol{M}^+(\theta,\phi)\,(i\boldsymbol{\omega}(\theta,\phi) + \boldsymbol{T}_2 + \boldsymbol{\Pi}) \tag{2.11}$$

where $\boldsymbol{M}^+(\theta,\phi;t)$ is a vector of dimension N, whose components are the transverse magnetizations of the exchanging sites. $\boldsymbol{\omega}$ is a diagonal matrix of dimension $N \times N$

containing the resonance frequencies of each site. The matrix $\mathbf{\Pi}$ describes the exchange of magnetization between the N sites following the discrete jumps model. The matrix elements have the form:

$$\Pi_{ij} = \Omega_{ij} p_j \qquad \text{e} \qquad \Pi_{ii} = -\sum_{j(\neq i)}^{N} \Pi_{ij} \tag{2.12}$$

where Ω_{ij} is the inverse of the correlation time of the jump between the site i and j, and p_j is the population of site j.

Similarly to the static case, the solution of equation 2.11 is:

$$\begin{aligned} \boldsymbol{M}^{+}(t) &= \frac{1}{8\pi^2} \int_0^{2\pi} \int_0^{\pi} \boldsymbol{M}_0^{+}(\theta,\phi) e^{(i\boldsymbol{\omega}(\theta,\phi)t + \boldsymbol{T}_2 + \mathbf{\Pi})} \; sin\theta \; d\theta \; d\phi \\ &= \frac{1}{8\pi^2} \int_0^{2\pi} \int_0^{\pi} \boldsymbol{M}_0^{+}(\theta,\phi) \boldsymbol{L}(\theta,\phi;t) \; sin\theta \; d\theta \; d\phi \end{aligned} \tag{2.13}$$

where the propagator $\boldsymbol{L}(\theta,\phi;t)$ is:

$$\boldsymbol{L}(\theta,\phi;t) = e^{(i\boldsymbol{\omega}(\theta,\phi)t + \boldsymbol{T}_2 + \mathbf{\Pi})} \tag{2.14}$$

$\boldsymbol{L}(\theta,\phi;t)$ is calculated by diagonalizing the matrix $(i\boldsymbol{\omega}(\theta,\phi)t + \boldsymbol{T_2} + \mathbf{\Pi})$. The exponential of equation 2.14 can be expressed with the eigenvectors $\boldsymbol{V}$ and eigenvalues $\boldsymbol{A}$:

$$\boldsymbol{L}(\theta,\phi;t) = \boldsymbol{V}^{-1} e^{\boldsymbol{A}} \boldsymbol{V} \tag{2.15}$$

Since $\boldsymbol{A}$ is diagonal, $exp(\boldsymbol{A})$ is diagonal as well, and its elements are $exp(A_{ij})$.

The dependence of the powder lineshape on the frequency of an aromatic ring π-flip for the chemical shift and quadrupolar interactions is shown if fig. 2.2 in the case of ^{13}C and ^{2}H nuclei, respectively.

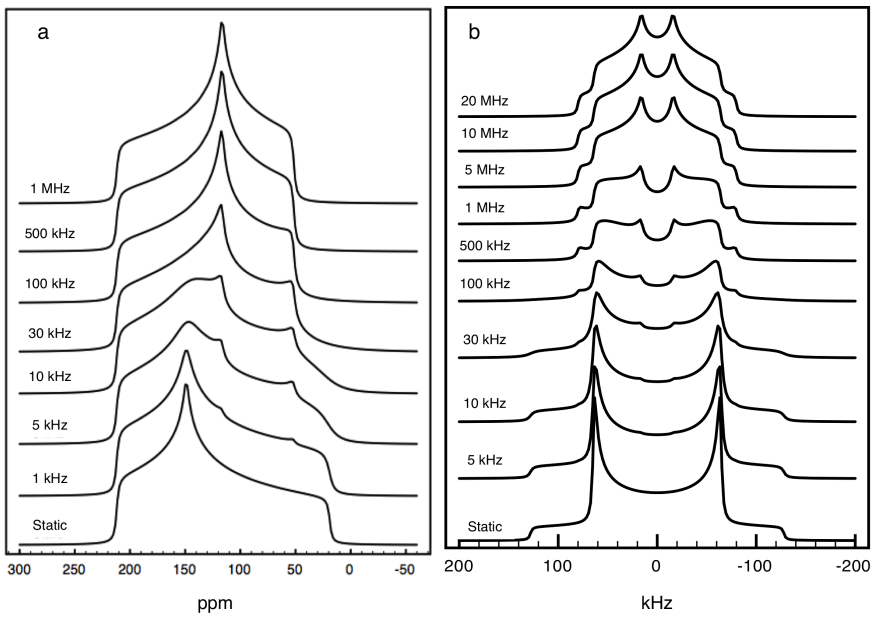

Figure 2.2: a) Effect of a π-flip on the powder CSA lineshape of a ternary aromatic carbon as a function of the motional frequency. a) Effect of a π-flip on the powder quadrupolar lineshape of a deuterium as a function of the motional frequency.

2.2.2 Fast motion limit lineshape

When the frequency of the molecular motion is much larger than the static linewidth, the lineshape is not sensitive to further increments of the motional frequency. If this condition is achieved, the system is said to be in the *fast motion limit*. The calculation of the powder pattern in this limit, within the Markov model, is particularly simple. In this condition, the interaction is governed by an average tensor, which does not dependent on the frequency of the motion.

The average tensor of the chemical shift interaction, for example, expressed in an axes frame fixed on the crystal lattice, is:

$$\boldsymbol{\sigma}_{avg}^{cryst} = \sum_{i}^{N} p_i \boldsymbol{\sigma}_i^{cryst} \tag{2.16}$$

where p_i is the population of each site, and $\boldsymbol{\sigma}_i^{cryst}$ is the interaction tensor for the site i. In this case, the lineshape simulation is performed as for the general static case, with the only difference that the interaction tensor is substituted with $\boldsymbol{\sigma}_{avg}^{cryst}$.

2.3 Relaxation and dynamics

Molecular motions cause a time dependence of nuclear spin interactions. As discussed before, this affects the lineshape of the signals, and also determines the relaxation mechanisms. The relaxation process is comparable to the excitation one: the latter is a transition induced by radiofrequency pulses, where the radiation responsible for the excitation is the oscillating magnetic field B_1; relaxation is induced by the nuclear spin interactions, which, modulated by molecular motions, produce fluctuating local magnetic fields.

Since molecular motions and the produced fluctuating fields are non-coherent processes, they can be described by an autocorrelation function (Eq. 2.1), which, as already mentioned, has a decreasing trend with increasing τ. The calculation of spin-lattice relaxation rates involves an analysis of the fluctuating magnetic fields

in order to determine the available power for the corresponding transitions.

If the autocorrelation function is exponential (equation 2.2), it can be written in the form:

$$G(\tau) = \overline{b(t)b(t+\tau)} = \langle b^2 \rangle_{eq} exp\left(-\frac{|\tau|}{\tau_c}\right) \tag{2.17}$$

where $\langle b^2 \rangle_{eq}$ is the average of the squared instantaneous magnetic field, over the particles of the system.

The Fourier transform of the autocorrelation function 2.17 is called *spectral density* and it is a Lorentzian function:

$$J(\omega) = \langle b^2 \rangle_{eq} \frac{2\tau_c}{1 + \omega^2 \tau_c^2} \tag{2.18}$$

The trend of this function (Figure 2.3) indicates that the available power is almost constant with the logarithm of the frequency until a certain value of $\omega \simeq \tau_c^{-1}$, after this value it decays as $(\omega^2 \tau_c^2)^{-1}$.

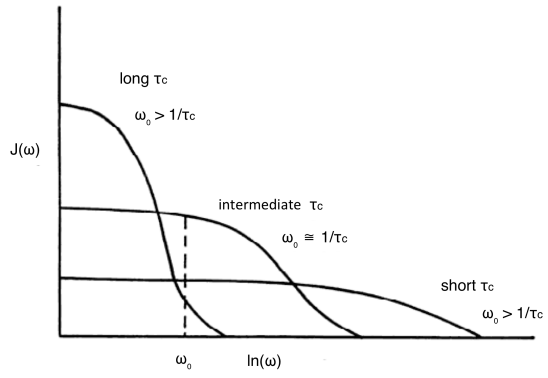

Figure 2.3: Trend of the spectral density as a function of $ln(\omega)$.

Following the Redfield theory [20], the *relaxation rates* are expressed as linear combinations of spectral densities:

$$R_j = (T_j)^{-1} = \sum_{i=1}^{n} a_i J(\omega_i) \tag{2.19}$$

where a_i is the coefficient relative to the spectral density at ω_i, and j indicates the involved relaxation mechanism, with $j = 1, 1\rho, 2$.

The most intense nuclear spin interactions are the quadrupolar and dipolar ones. Relaxation of quadrupolar nuclei, for which the main relaxation mechanism is the fluctuation of the quadrupolar interaction, will not be treated in the present thesis. For spins $I = \frac{1}{2}$, relaxation mainly occurs through the dipolar mechanism.

Transverse and longitudinal relaxation times have a different dependence on spectral density and must be treated independently. In particular, some characteristics of T_2 relaxation in the solid state needs to be specified.

2.3.1 Spin-spin relaxation in the solid state

The FID (Free Induction Decay) of solid samples is generally very short (decaying typically in tents of microseconds). Therefore, if we define T_2 as a time constant describing the decay of transverse magnetization, in solids T_2 will be several orders of magnitude shorter than liquids. Moreover the meaning and the interpretation of T_2 in solids are very different with respect to those of T_2 in liquids. First of all the decay of the transverse magnetization in solids is often non-exponential therefore making non-straightforward even the identification of T_2. Furthermore, while in liquids T_2 is determined by molecular motions and, to some extent, by magnetic field inhomogeneity, in solids it is typically determined by residual anisotropic interactions. For example, ^{1}H T_2 values, determined in static conditions, are a measurement of the residual homonuclear dipolar interaction, *i.e.* the average of the "static" interaction operated by molecular motions.

For these reasons, T_2 in solid samples does not obey to equations similar to those used for liquid samples. Nevertheles its value is itself a measurement of the mobility of the solid phase. With increasing temperature (and consequently

the frequencies of molecular motions) T_2 monotonically increases (Figure 2.4). Each motion contributes to increase the T_2 value by a fixed amount depending on its efficiency in averaging the dominant interaction present, and therefore on the geometry of the motion itself. For example, the activation of a methyl rotation about its symmetry axis leads to a small increase of T_2, even though at very large motional frequency. In particular, T_2 values are basically independent of temperature when the frequency of the motion (ν) is much smaller or larger than the width of the static powder pattern (Δ) expressed in frequency units, while there is a region of maximum sensitivity, when $\nu \simeq \Delta$, in which T_2 jumps from the initial value to the one determined by the residual interaction.

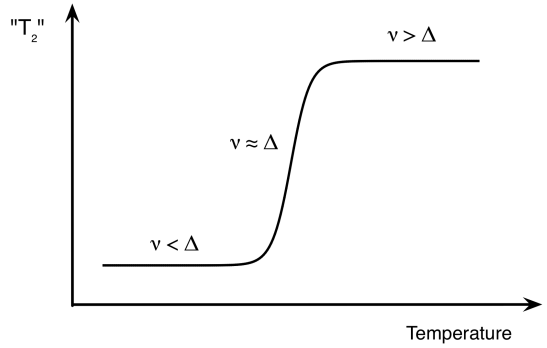

Figure 2.4: Trend of solid T_2 with temperature. The effect of a single molecular motion is shown: the three region of the graphic represent the regimes in which the frequency of the motion (ν) is smaller, of the same order, or larger than the width of the static powder pattern (Δ) expressed in frequency units.

2.3.2 Spin-lattice relaxation driven by homonuclear dipolar coupling

The homonuclear dipolar coupling is generally responsible for relaxation of abundant nuclei. In the majority of the cases we deal with protons as abundant nuclei, which are present in all the organic systems and in many inorganic ones, but the following treatment can be also applied to ^{19}F nuclei in perfluorinated systems.

Longitudinal relaxation time of abundant nuclei: $T_1(^1H)$

Spin-lattice relaxation time values contain direct dynamic information, since this relaxation mechanism directly depends on the modulation of the dipolar interactions: if the modulation frequency is of the same order of magnitude of the Larmor frequency, the mechanism is effective and the relaxation rate values are high (small T_1 values). If a single molecular motion is taken into account, the general expression for the relaxation rate of a pair of nuclei interacting through homonuclear dipolar coupling is [7]:

$$R_1 = T_1^{-1} = \frac{3}{2} K_I \left[J(\omega_0) + 4\ J(2\omega_0) \right] \tag{2.20}$$

where K_I is calculated as:

$$K_I = \left(\frac{\mu_0}{4\pi} \right)^2 \frac{\gamma^4}{r^6} \hbar^2 I(I+1) \tag{2.21}$$

with r the internuclear H-H distance. $J(\omega)$ are the spectral densities under the assumption that the same function is valid for the different order of J (1 or 2), coming form the rank-2 dipolar tensor. This assumption is retained in the following treatment.

If more than two coupled protons are present in the sample, in equation 2.20 the value of K_I changes and in general its analytical expression is much more complicated, since it takes into account the geometry of all the different couplings. The relaxation rate can be written as follows:

$$R_1 = T_1^{-1} = \frac{3}{2} C_H \left[J(\omega_0) + 4\ J(2\omega_0) \right] \tag{2.22}$$

where C_H is a numerical constant, not known in principle, and generally determined as a fitting parameter.

Longitudinal relaxation time in the rotating frame of abundant nuclei: $T_{1\rho}(^1H)$

Spin-lattice relaxation in the rotating frame is similar to that in the laboratory frame (T_1). In the case of relaxation of abundant nuclei, driven by the homonuclear dipolar interaction, this kind of relaxation only depends on the modulation operated by molecular motions, thus containing pure dynamical information. This relaxation mechanism is sensitive to motions with frequencies of the order of the spin lock frequency (20-100 kHz). In the expression describing the spin-lattice relaxation in the rotating frame, a term of the spectral density depending on the spin lock frequency (ω_1) appears [21]:

$$R_{1\rho} = T_{1\rho}^{-1} = C_H \left[\frac{3}{10} J(2\omega_1) + \frac{1}{2} J(\omega_0) + \frac{1}{5} J(2\omega_0) \right] \tag{2.23}$$

written for n coupled protons, and with $C_H = K_I$ when n=2.

The study of longitudinal relaxation times of abundant nuclei is a tool for obtaining global dynamic information. In fact, it is true that the intrinsic T_1 and $T_{1\rho}$ values of protons belonging to a particular molecular fragment depend on motion of the specific fragment, but the effect of spin diffusion has to be taken into account. Indeed, abundant nuclei often form a network of strong homonuclear couplings connecting all the nuclei of the sample. In these conditions T_1 and $T_{1\rho}$ values are averaged by spin diffusion either to a single value or to partially averaged components. In both these cases site-specific information are lost because the intrinsic components cannot be measured. When a single value is experimentally obtained, it contains the contributions of all the molecular motions of the sample that are effective for the kind of relaxation considered. The relaxation rate can be expressed as a sum of the spectral densities of the different motions.

$$R_x = \sum_i R_x^i \tag{2.24}$$

where $x = 1$ or 1ρ, R_x^i are given by equation 2.22 and 2.23, for T_1 and $T_{1\rho}$, respectively, and i runs over the molecular motions.

When partially average components are measured, dynamic information can be obtained by calculating the population-weighted rate average (PWRA) quantity, which is independent from spin diffusion [22, 23]:

$$PWRA = \sum_l \frac{w_l}{T_l} \tag{2.25}$$

where T_l and w_l are the values and the weight of the measured components. The PWRA value can be treated as the completely averaged T_x value.

2.3.3 Spin-lattice relaxation driven by heteronuclear dipolar coupling

The heteronuclear dipolar interaction plays a fundamental role in the relaxation processes of rare nuclei, because the most intense interaction they are subjected to is the dipolar coupling with the abundant nuclei bonded to them. In organic system and especially in the pharmaceutical field, the most studied rare nuclei are ^{13}C, ^{15}N, ^{29}Si, ^{31}P; all these nuclei generally have strong dipolar coupling with directly bonded protons (or ^{19}F nuclei in perfluorinated system).

Longitudinal relaxation time of rare nuclei: $T_1(^{13}C)$

The fluctuation of the dipolar interaction between two nuclei I and S, resonating at ω_I and ω_S respectively, causes the spin-lattice relaxation. The two longitudinal magnetizations (M_Z^I, M_Z^S) are coupled, and their evolution can be expressed by the Solomon equations:

$$\begin{aligned} \frac{dM_Z^I}{dt} &= R_1^{II}\Delta M_Z^I + R_1^{IS}\Delta M_Z^S \\ \frac{dM_Z^S}{dt} &= R_1^{SI}\Delta M_Z^I + R_1^{SS}\Delta M_Z^S \end{aligned} \tag{2.26}$$

where $\Delta M_Z^\lambda = M_0^\lambda - M_Z^\lambda(t)$ $(\lambda = I, S)$ and the spin-lattice relaxation rates are of the form:

$$\begin{aligned} R_1^{II} = (T_1^{II})^{-1} &= \frac{K'}{15}\left[J(\omega_I - \omega_S) + 3\ J(\omega_I) + 6\ J(\omega_I + \omega_S)\right] \\ R_1^{IS} = (T_1^{IS})^{-1} &= \frac{K'}{15}\left[-J(\omega_I - \omega_S) + 6\ J(\omega_I + \omega_S)\right] \end{aligned} \tag{2.27}$$

R_1^{SS} and R_1^{SI} are obtained from the same equations (2.27) exchanging the indexes I and S; K', similarly to the homonuclear case, results:

$$K' = \left(\frac{\mu_0}{4\pi}\right)^2 \frac{\gamma_I^2\gamma_S^2}{r^6}\hbar^2 I(I+1) \tag{2.28}$$

where r is the internuclear I-S distance.

The *homo-relaxation* rates R_1^{II} and R_1^{SS} contain spectral density terms at frequencies equal to the sum and the difference of ω_I and ω_S, in addition to the terms depending on their own Larmor frequency. The dependence on the sum and the difference of the two frequencies arises from the $\hat{I}^+\hat{S}^- + \hat{I}^-\hat{S}^+$ e $\hat{I}^-\hat{S}^-/\hat{I}^+\hat{S}^+$ terms of the dipolar Hamiltonian; these terms are the sole responsible for *cross-relaxation* (R_1^{IS} and R_1^{SI}).

In the thesis work particular attention was dedicated to relaxation of ^{13}C. For this nucleus the heteronuclear dipolar coupling is the principal relaxation mechanism, and the other interactions are neglected in the treatment. The T_1 of a ^{13}C nucleus bonded to N equivalent protons, with a constant bond length r_{CH} is expressed through the following equation [24]:

$$R_1(^{13}\mathrm{C}) = (T_1(^{13}\mathrm{C}))^{-1} = \frac{N}{15}K'\left[J(\omega_H - \omega_C) + 3\ J(\omega_C) + 6J(\omega_H + \omega_C)\right] \tag{2.29}$$

This treatment assumes that the only significative couplings are those with the directly bonded protons and that the *cross-relaxation* terms are negligible. When these conditions are not verified, different and more complex approaches are needed.

Longitudinal relaxation time in the rotating frame of rare nuclei: $T_{1\rho}(^{13}C)$

Contrary to $T_{1\rho}$ of abundant nuclei, the longitudinal relaxation time in the rotating frame of ^{13}C nuclei, is not directly interpretable in terms of dynamic processes, because, along with a spin-lattice contribution depending only on dynamics, it also contains a spin-spin contribution. This term derives from flip-flop mechanisms occurring between ^{13}C and ^{1}H nuclei, which get *in contact* under the effect of the spin lock field.

In a paper published in 1979 VanderHart and Garroway [25] examined the conditions for which the observed $T_{1\rho}$ is principally determined by molecular motions, and when the spin-spin contribution is dominant. For rigid crystalline solids, with a network of strongly coupled protons, and if the MAS frequency is not very high, the spin-spin contribution is often non-negligible. This was previously demonstrated for crystalline Ibuprofen [26] and since the systems studied in the thesis data are similar, $T_{1\rho}(^{13}C)$ and their trend with temperature were not included in the data analysis.

2.3.4 Models for spectral densities

In order to give an analytical expression for the spectral densities, theories that provide motional models are required. In the next paragraphs the simplest model (BPP) and the Cole-Cole model are described.

BPP theory

In the theory elaborated by Bloembergen, Purcell and Pound in 1948 (BPP) [27], the motion is assumed to be isotropic, with the internuclear distance $|r_k|$ kept constant during the motion; another assumption is that the same exponential autocorrelation function determines all the orders of $J^{(n)}(\omega)$. Under these hypothesis, the spectral densities are expressed as Lorentzian functions and, as used in the previous paragraph, if the multiplicative coefficients are explicit in the relaxation rate expression, the expression for $J^{BPP}(\omega)$ is.

$$J^{BPP}(\omega) = \frac{2\tau_c}{1+\omega^2\tau_c^2} \tag{2.30}$$

Within the BPP model, for an ensemble of nuclei of the same species, for example ^{1}H, and taking into account a single motion the expression for spin lattice relaxation rates results [24]:

$$R_1 = T_1^{-1} = \frac{3}{2}C_H\left(\frac{\tau_c}{1+\omega_0^2\tau_c^2} + \frac{4\tau_c}{1+4\omega_0^2\tau_c^2}\right) \tag{2.31}$$

$$R_{1\rho} = T_{1\rho}^{-1} = C_H\left[\frac{3}{10}\left(\frac{\tau_c}{1+4\omega_1^2\tau_c^2}\right) + \frac{1}{2}\left(\frac{\tau_c}{1+\omega_0^2\tau_c^2}\right) + \frac{1}{5}\left(\frac{\tau_c}{1+4\omega_0^2\tau_c^2}\right)\right] \tag{2.32}$$

The trends of the relaxation rates with the correlation time of the motions are shown in Figure 2.5.

Following the BPP theory the expression for relaxation rates of rare nuclei dipolarly coupled to abundant nuclei, as a function of both the Larmor frequencies and of the correlation time is given by the following equation (as an example the common case of ^{1}H and ^{13}C nuclei is considered):

$$R_1(^{13}\mathrm{C}) = (T_1(^{13}\mathrm{C}))^{-1} = \frac{N}{15}K'\left[\frac{\tau_c}{1+(\omega_H-\omega_C)^2\tau_c^2} + \frac{3\tau_c}{1+\omega_C^2\tau_c^2} + \frac{6\tau_c}{1+(\omega_H+\omega_C)^2\tau_c^2}\right] \tag{2.33}$$

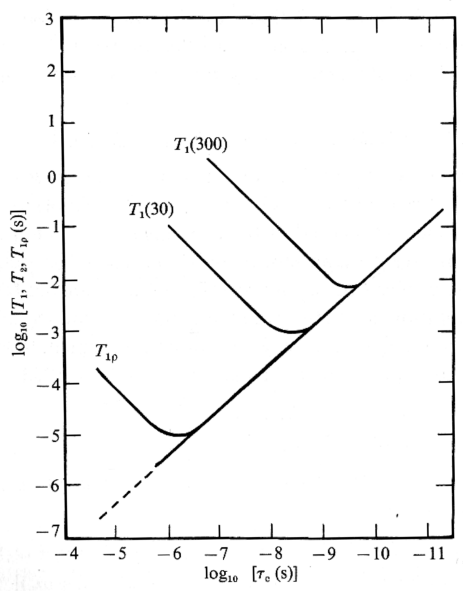

Figure 2.5: Trends of proton relaxation times, T_1, $T_{1\rho}$ as a function of correlation time of the motion responsible for relaxation. Both the axes have a logarithmic scale.

The trend of $T_1(^{13}C)$, within the BPP model, as a function of the correlation time is shown in Figure 2.6 (case $\delta = 0$).

The BPP theory is not always appriopriate to solid systems, as it is based on the assumption of isotropic motion, which is not always applicable for molecular motions occurring in the solid state. In some cases more complex models, which can include correlation effects between different motions or distributions of characteristic times, are necessary [28].

Cole-Cole spectral density

The Cole-Cole (CC) model takes into account the possible correlation of the motions. The mathematical expression of the spectral density within this model is:

$$J_{CC}(\omega) = \frac{2}{\omega} sin\left(\frac{\delta\pi}{2}\right)\left[\frac{(\omega\tau)^{\delta}}{1+(\omega\tau)^{2\delta}+[2cos(\delta\pi/2)](\omega\tau)^{\delta}}\right] \tag{2.34}$$

The parameter δ characterizes the extent of the correlation: $\delta = 1$ means a unique activation energy and no correlated motion, whereas $\delta = 0$ implies the maximum distribution of activation energies and a considerable degree of correlated motion. The slow ($\omega\tau \gg 1$) and fast ($\omega\tau \ll 1$) motion limits are described by the following equations:

$$J_{CC}(\omega) = \frac{2}{\omega}\left[sin\left(\frac{\delta\pi}{2}\right)\right]\tau^{-\delta}\omega^{-(1+\delta)} \ , \quad \omega\tau \gg 1 \ ; \tag{2.35}$$

and

$$J_{CC}(\omega) = \frac{2}{\omega}\left[sin\left(\frac{\delta\pi}{2}\right)\right]\tau^{\delta}\omega^{-(1-\delta)} \ , \quad \omega\tau \ll 1 \ ; \tag{2.36}$$

and the slopes of $ln(J_{CC})$ vs. $ln(\tau)$ in the two regimes are $-\delta$ and $+\delta$, respectively. The trend of T_1 relaxation times for nuclei ^{1}H and ^{13}C as a function of the correlation time of the motion responsible for relaxation, calculated within the Cole-Cole model are plotted in Figure 2.6.

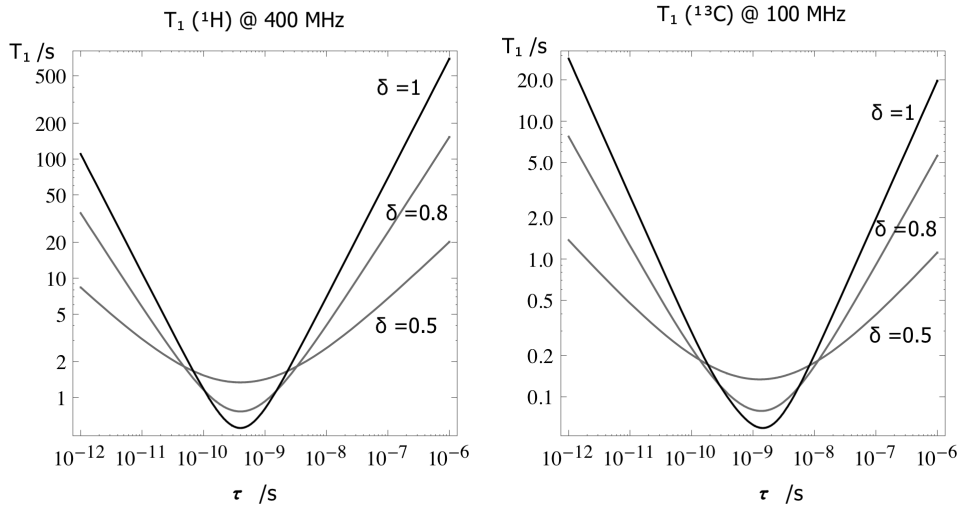

Figure 2.6: T_1 relaxation times (for ^{1}H and ^{13}C nuclei) trends with correlation time of the motion responsible for relaxation, in the case of Cole-Cole spectral density (δ values are indicated on each curve). Both the axes have a logarithmic scale.

2.3.5 Relaxation of methyl groups: the effects of classical motions and quantum tunneling

The mechanism of reorientation of CH_3 groups in solids has been investigated by NMR since the 1950's [29, 30] and the quantum tunneling rotation was considered in the following years [31, 32]. A rigorous treatment of the theory about the quantum tunneling aspects is out of the scope of this thesis, in this paragraph the autocorrelation functions describing the motions consisting of jumps over the barrier (classical motion) and jumps through the barriers (incoherent tunneling) proposed by Latanowicz [33] are shown, referring to the literature for theoretical details (see in particular ref. [34] and references therein).

For methyl protons, the expression of R_1 as linear combination of spectral densities is of the form:

$$R_1 = \frac{1}{T_1} = C_H \left[J^1(\omega_0 + \omega_T) + J^1(\omega_0 - \omega_T) + J^2(2\omega_0 + \omega_T) + J^2(2\omega_0 - \omega_T) \right] \tag{2.37}$$

where $\omega_0 \pm \omega_T$ and $2\omega_0 \pm \omega_T$ replace ω_0 and $2\omega_0$ in the spectral density describing the sole classical motion. $\hbar\omega_T$ is the tunneling splitting, and the spectral densities J^1 and J^2 are of the form [33]:

$$J^1(\omega) = \frac{2}{15}\left[\frac{2\tau_c^H}{1+(\omega\ \tau_c^H)^2} + \frac{2\tau_c^T}{1+(\omega\ \tau_c^T)^2}\right] + \frac{6}{15}\frac{2\tau_c^{HT}}{1+(\omega\ \tau_c^{HT})^2} \tag{2.38}$$

$$J^2(\omega) = \frac{8}{15}\left[\frac{2\tau_c^H}{1+(\omega\ \tau_c^H)^2} + \frac{2\tau_c^T}{1+(\omega\ \tau_c^T)^2}\right] + \frac{16}{15}\frac{2\tau_c^{HT}}{1+(\omega\ \tau_c^{HT})^2} \tag{2.39}$$

where τ_c^H is the correlation time of the classical motion, τ_c^T is that of the quantum tunneling and τ_c^{TH} is given by the relation [33]:

$$\frac{1}{\tau_c^{TH}} = \frac{1}{\tau_c^H} + \frac{1}{\tau_c^T} \tag{2.40}$$

The temperature dependence of τ_c^H is given by the Arrhenius law:

$$\tau_c^H = \tau_\infty^H \, e^{\frac{E_a}{RT}} \tag{2.41}$$

While the temperature dependence of τ_c^T was proposed in ref. [35] and is of the following form:

$$\tau_c^T = \tau_\infty^T \, e^{B\sqrt{E_a - Cp\ T}} \tag{2.42}$$

The value of B depends on the mass of the tunneling particle and on the width of the potential barrier. For geometrical parameters typical of the CH_3 group $B = 0.25\ (J^{-\frac{1}{2}})$.